Inactivating peptide of the *Shaker* B potassium channel: conformational preferences inferred from studies on simple model systems

José A. ENCINAR*, Asia M. FERNÁNDEZ*, Emilio GIL-MARTÍN*, Francisco GAVILANES†, Juan P. ALBAR‡, José A. FERRAGUT* and José M. GONZÁLEZ-ROS[1]*

*Departamento de Neuroquímica, Universidad Miguel Hernández, Campus de Elche, 03206 Elche (Alicante), Spain, †Departamento de Bioquímica, Facultad de Ciencias Químicas, Universidad Complutense, 28040 Madrid, Spain, and ‡Centro Nacional de Biotecnología, CSIC, Departamento de Inmunología y Oncología, Cantoblanco, 28049 Madrid, Spain

Previous studies on the interaction between the inactivating peptide of the *Shaker* B K^+ channel (ShB peptide, H_2N-MAAVAGLYGLGEDRQHRKKQ) and anionic phospholipid vesicles, used as model targets, have shown that the ShB peptide: (i) binds to the vesicle surface with high affinity; (ii) readily adopts a strongly hydrogen-bonded β-structure; and (iii) becomes inserted into the hydrophobic bilayer. We now report fluorescence studies showing that the vesicle-inserted ShB peptide is in a monomeric form and, therefore, the observed β-structure must be intramolecularly hydrogen-bonded to produce a β-hairpin conformation. Also, additional freeze–fracture and accessibility-to-trypsin studies, which aimed to estimate how deeply and in which orientation the folded monomeric peptide inserts into the model target, have allowed us to build structural models for the target-inserted peptide. In such models, the peptide has been folded near G6 to configure a long β-hairpin modelled to produce an internal cancellation of net charges in the stretch comprising amino acids 1–16. As to the positively charged C-terminal portion of the ShB peptide (RKKQ), this has been modelled to be in parallel with the anionic membrane surface to facilitate electrostatic interactions. Since the negatively charged surface and the hydrophobic domains in the model vesicle target may partly imitate those present at the inactivation 'entrance' in the channel protein [Kukuljan, M., Labarca, P. and Latorre, R. (1995) Am. J. Physiol. Cell Physiol. **268**, C535–C556], we believe that the structural models postulated here for the vesicle-inserted peptide could help to understand how the ShB peptide associates with the channel during inactivation and why mutations at specific sites in the ShB peptide sequence, such as that in the ShB-L7E peptide, result in non-inactivating peptide variants.

INTRODUCTION

Early studies on the rapid inactivation exhibited by many voltage-dependent ion channels specific for Na^+ or K^+ envisioned this process to be a consequence of the physical occlusion of the channel's internal mouth by a flexible cytoplasmic domain of the channel protein itself, which acts as an open-channel blocker (the 'ball and chain' hypothesis of channel inactivation [1]). More recently, such a hypothesis has received strong experimental support and indeed, molecular identification of the current-inactivating 'ball' peptide, its connecting polypeptide 'chain', the receptor site for the ball on the channel protein and the mechanisms determining their mutual interactions, are being pursued.

In the *Shaker* B (ShB) K^+ channel [2,3], the inactivating ball peptide (ShB peptide) corresponds to the first 20 amino acids in the N-terminal region of each of the four approx. 70 kDa ShB channel subunits (H_2N-MAAVAGLYGLGEDRQHRKKQ) [4–6]. These ShB ball peptides are tethered to the rest of the channel protein by a 200 amino acid-long hydrophilic polypeptide that constitutes the chain polypeptide. Besides its role in maintaining each ball peptide near its receptor site on the cytoplasmic mouth of the channel, part of the chain (amino acids 83–196), which is highly conserved in all *Shaker* variants and related channels, constitutes the minimal structural element responsible for oligomerization of compatible subunits to form functional channels [7]. This raises the possibility that the N-terminal ball could also be involved in oligomerization and so it is conceivable that the functional inactivating ball results from co-assembly of several individual ball peptides in the tetrameric ShB K^+ channel. Nonetheless, in strong opposition to such a possibility, MacKinnon et al. [8] and Gomez-Lagunas and Armstrong [9] have concluded that the four ball peptides in the ShB channel behave independently, each causing channel inactivation in a mutually exclusive manner. These results suggest that the functional ball can be configured from a single ShB peptide which, therefore, it is not subjected to oligomerization.

A remarkable finding that followed the identification of the ball peptide in the ShB K^+ channel was that a synthetic peptide derived from the ShB peptide sequence also serves as an inactivating ball for a variety of other voltage-dependent K^+ channels [3,10,11], high-conductance Ca^{2+}-activated K^+ channels [12,13] or cyclic-nucleotide-gated channels [14], some of which do not normally inactivate. Similarly, putative ball peptides derived from the sequences of *Shaker* C and *Shaker* D channels, as well as from the mammalian homologue *raw*3, are efficient blockers of the ShB K^+ channel, despite the lack of conservation of primary structure [15]. Furthermore, the presumed inactivating

Abbreviations used: ShB, *Shaker* B; ShB K^+ channel, splicing variant B of the rapidly inactivating, voltage-dependent K^+ channels coded in the *Shaker* locus of *Drosophila*; ShB peptide, the inactivating peptide of the ShB K^+ channel; NBD, *N*,*N*′-dimethyl-*N*-(iodoacetyl)-*N*′-(7-nitrobenz-2-oxa-1,3-diazol-4-yl)ethylenediamine; rho, tetramethylrhodamine-5-iodoacetamide; pyr, *N*-(1-pyrene)iodoacetamide; PC, phosphatidylcholine from egg yolk; PA, phosphatidic acid derived from egg yolk PC; FTIR, Fourier-transform IR spectroscopy; IMPs, intramembrane particles.

[1] To whom correspondence should be addressed (e-mail gonzalez.ros@umh.es).

peptide from the voltage-dependent Na^+ channel also inactivates the ShB K^+ channel [16]. From the above crossed-inactivation phenomena, it has been concluded that the molecular-recognition events leading to the formation of the inactivating peptide–channel complex and, therefore, to channel inactivation, have a rather unconstrained basis in terms of primary structure and that there are two relevant domains configuring the receptor site for the inactivating peptide in the channel protein: (i) a hydrophobic pocket, which becomes accessible only upon channel opening, separated from the cytoplasm by (ii) a region with a negative surface potential [4,6,17].

Attempting to gain insight into the molecular events in which the inactivating peptide might be involved during channel inactivation, we previously reported on the use of anionic phospholipid vesicles as a model target that partly imitates the corresponding domains in the channel's receptor site for the inactivating peptide, as it also contains a region with a negative surface potential (the negatively charged vesicle surface) and a hydrophobic domain (the lipid bilayer) [18,19]. In this paper we have determined that the ShB peptide inserts into such a model target in a monomeric form to configure an intramolecular β-hairpin structure. Also, additional studies, aimed at determining how deeply and in which orientation the folded monomeric peptide inserts into the model target, have allowed us to build structural models for the target-inserted peptide, which seem compatible with the experimental results obtained so far on this subject.

MATERIALS AND METHODS

Peptide synthesis and characterization

The wild-type ShB peptide (MAAVAG**L**YGLGEDRQHRK-KQ) and the non-inactivating mutant peptide ShB-L7E (MA-AVAG**E**YGLGEDRQHRKKQ; where bold shows nucleotides that vary) [2] were synthesized as C-terminal amides on an automatic multiple synthesizer (AMS 422, Abimed, Lanfengeld, Germany) using a solid-phase procedure and standard Fmoc-chemistry [18]. The peptides were purified by reverse-phase HPLC to better than 95% purity and their composition and molecular mass were confirmed by amino acid analysis and MS, respectively [18]. Residual trifluoroacetic acid used both in the peptide synthesis and in the HPLC mobile phase (trifluoroacetate has a strong IR absorbance at 1673 cm^{-1}, which interferes with the characterization of the peptide amide I band [20]), was removed by several lyophilization–solubilization cycles in 10 mM HCl [21].

Fluorescent labelling of cysteine-containing peptides

The peptides ShB-21C (MAAVAG**L**YGLGEDRQHRKKQ**C**) and ShB-L7E-21C (MAAVAG**E**YGLGEDRQHRKKQ**C**) were synthesized as C-terminal amides as described above for the ShB and ShB-L7E peptides. These cysteine-containing peptides were fluorescently labelled by alkylation of their C-terminal sulphydryl group with either NBD [*N*,*N*′-dimethyl-*N*-(iodoacetyl)-*N*′-(7-nitrobenz-2-oxa-1,3-diazol-4-yl)ethylenediamine] [19], rho (tetramethylrhodamine-5-iodoacetamide) or pyr [N-(1-pyrene)iodoacetamide] (Molecular Probes, Eugene, OR, U.S.A.). Briefly, lyophilized 1–3 mg aliquots of either cysteine peptide were dissolved in 0.6 ml of 0.5 M Tris buffer, pH 8.5, reacted for 1 h in the dark with a 4-fold molar excess of the reducing agent dithiothreitol and alkylated by addition of an excess of the corresponding fluorophore-iodoacetamide (2.5-fold molar excess over the dithiothreitol) dissolved in DMSO. The reaction mixtures were incubated for 1 h in the dark under an inert atmosphere, then subjected to chromatography in a Biogel P-2 (Fine) column with 0.2 M ammonium acetate as the eluant. The resulting fluorescently labelled peptides (Table 1) eluted in the void volume and were subsequently lyophilized, re-chromatographed, divided into aliquots, lyophilized again and kept frozen. Peptide concentration was determined by amino acid analysis. The extent of derivatization was estimated by determining the carboxymethylcysteine/peptide molar ratios in the labelled peptide samples (Table 1).

Preparation of small unilamellar phospholipid vesicles

The phospholipids phosphatidylcholine (PC) and phosphatidic acid (PA) (Avanti Polar Lipids, Birmingham, AL, U.S.A.) used in these studies were derived from egg-yolk PC and, therefore, have the same fatty acid composition as egg-yolk PC. The lyophilized phospholipids were dissolved in chloroform, divided into aliquots and the solvent was driven off under a stream of nitrogen and under a vacuum. The resulting dry lipid films were suspended in the required buffer at concentrations up to 3 mM in terms of lipid phosphorus [22], frequently vortexed and sonicated in a bath-type sonicator until the samples became completely transparent.

Fluorescence measurements

Samples for fluorescence resonance energy transfer measurements were prepared from stock solutions of fluorescently labelled peptides and small unilamellar PA vesicles in 10 mM Hepes

Table 1 Amino acid sequences of ShB peptides (as C-terminal amides) and their fluorescently labelled analogues

Peptide	Peptide designation	Extent of derivatization	Peptide sequence (1 5 10 15 20)
1	ShB		M A A V A G L Y G L G E D R Q H R K K Q
2	ShBL7E		M A A V A G **E** Y G L G E D R Q H R K K Q
3	ShB-Cys		M A A V A G L Y G L G E D R Q H R K K Q C
4	ShBL7E-Cys		M A A V A G **E** Y G L G E D R Q H R K K Q C
5	ShB-NBD	89%	M A A V A G L Y G L G E D R Q H R K K Q C-NBD
6	ShBL7E-NBD	88%	M A A V A G **E** Y G L G E D R Q H R K K Q C-NBD
7	ShB-Rho	76%	M A A V A G L Y G L G E D R Q H R K K Q C-Rho
8	ShBL7E-Rho	73%	M A A V A G **E** Y G L G E D R Q H R K K Q C-Rho
9	ShB-Pyr	75%	M A A V A G L Y G L G E D R Q H R K K Q C-Pyr
10	ShBL7E-Pyr	94%	M A A V A G **E** Y G L G E D R Q H R K K Q C-Pyr

buffer (pH 7.0)/100 mM NaCl to a final volume of 1.5 ml. The concentrations of the energy donors (either ShB-NBD or ShB-L7E-NBD peptides) and the energy acceptors (either ShB-rho or ShB-L7E-rho peptides) were maintained constant at 0.1 and 0.2 μM, respectively, while the concentration of PA vesicles ranged from 15 μM to 1.5 mM. Fluorescence emission spectra were obtained at room temperature in a SLM 8000 spectrofluorimeter with the excitation wavelength set at 450 nm. Although the excitation maximum for the NBD probe is 470 nm, a lower wavelength was chosen for these experiments to minimize the direct excitation of the accompanying rho-labelled peptides. The efficiency of energy transfer (E) was determined from the ratio of the fluorescence emitted at 530 nm (emission maximum of the donor NBD derivatives) in the presence (I_{da}) and in the absence (I_d) of the rho derivatives as the energy acceptors. To account for the background (scattering) signal contributed by the lipid vesicles to the emitted fluorescence, I_d was corrected by subtracting the signal observed when unlabelled peptides, at concentrations equal to the sum of the donor and acceptor derivatives, were added to the vesicles. Likewise, I_{da} was corrected for direct (non-energy transfer) acceptor emission by subtracting the fluorescence signal exhibited by vesicle samples containing the acceptor derivative alone, in the absence of donor. The percentage value of E is given by $E = [1-(I_{da}/I_d)] \times 100$.

The samples to examine pyrene excimer formation were prepared similarly, but using pyr-labelled ShB or ShB-L7E peptides (final concentration 0.3 μM) and small unilamellar PA vesicles (final concentration ranging from 30 μM to 1.5 mM). The emission spectra were obtained by exciting at the pyrene excitation maximum of 345 nm. Pyrene emission was corrected for vesicle scattering by subtracting the signal observed when 0.3 μM of unlabelled peptides were mixed with the same amounts of PA vesicles.

Freeze–fracture

Either ShB or ShB-L7E peptides (90 μM) were added to small unilamellar vesicles (0.7 mM in terms of lipid phosphorus) prepared from either egg PC or PA in 5 mM Hepes buffer, pH 7.0, containing 130 mM KCl and 20 mM NaCl. The peptide/vesicle mixtures were incubated for 30 min at room temperature, centrifuged at 255000 ***g*** for 6 h, and the supernatants were discarded and the pellets fixed by addition of 1 ml of buffer, containing 1% glutaraldehyde and 1% paraformaldehyde, for 30 min. Fixed samples were washed several times with buffer, soaked for 2 h in buffer containing 20% glycerol, coated with polyvinyl alcohol, frozen in Freon 22, fractured at −110 °C and shadowed with platinum/carbon in a Balzers 400 D apparatus. From each pellet, 3–6 replicas were prepared. Fracture faces were photographed in a Jeol 100B electron microscope.

Trypsin hydrolysis of peptide–vesicle complexes

ShB peptide (3.4 mM) and pre-formed small unilamellar PA vesicles (54 mM in terms of lipid phosphorus) were mixed to a final volume of 7 ml in 5 mM Hepes buffer, pH 7.0 (or alternatively pH 7.5), containing 20 mM NaCl and 130 mM KCl, and incubated for 10 min to allow the formation of peptide–vesicle complexes. Immobilized TPCK (L-1-tosylamido-2-phenylethylchloromethylketone)-trypsin (1 ml; Pierce, Rockford, IL, U.S.A.), previously washed in the above buffer, was added to the peptide–vesicle mixtures and incubated overnight at 37 °C. The digestion mixture was decanted from the immobilized trypsin gel, ultracentrifuged at 225000 ***g*** for 30 min to eliminate unbound peptide, and resuspended in buffer. The centrifugation–resuspension cycle was repeated twice and the final resuspended pellet divided into aliquots for either FTIR (Fourier-transform IR spectroscopy) or MS. Identical peptide–vesicle control samples prepared in the absence of trypsin, as well as samples of plain phospholipid vesicles, were similarly processed.

For IR spectroscopy, the aliquots were resuspended in buffer of identical saline composition but made from D_2O (deuterium oxide, 99.9% by atom, Sigma) to avoid the interference of H_2O IR absorbance (1645 cm^{-1}; [23]) in the peptide amide I band, centrifuged at 350000 ***g*** for 40 min, resuspended in 20 μl of D_2O buffer and placed into a liquid-demountable cell (Harrick, Ossining, NY, U.S.A.) equipped with CaF_2 windows and 50 μm thick mylar spacers. FTIR spectra were taken in a Nicolet 520 instrument equipped with a DTGS detector, as described [24]. No resolution-enhancement techniques were applied to the spectral data.

Aliquots for MS were simply lyophilized, dissolved in chloroform/methanol (2:1, by volume) and submitted to analysis in a Bruker (Bremen, Germany) Reflex II matrix-assisted laser desorption ionizing time-of-flight (MALDI-TOF) mass spectrometer, equipped with visualization optics and an N_2 laser (337 nm). A 20 μl volume of sample was mixed with 20 μl of a saturated solution of α-cyano-4-hydroxycinnamic acid (Sigma) used as a matrix. The mixture (1 μm) was deposited on a stainless-steel probe tip and left to dry at room temperature for 5 min prior to mass analysis. Mass spectra were recorded in linear positive mode at 28.5 kV acceleration voltage and 1.4 kV in the linear detector, by accumulating 40 spectra of single laser shots under threshold irradiance. The equipment was externally calibrated with a mixture of angiotensin (1047 Da) and insulin (5734 Da).

RESULTS

Fluorescence energy transfer and excimer formation studies of peptide self-association

Fluorescent derivatives of either the ShB or the ShB-L7E peptides have been shown previously to bind efficiently and in a saturable manner to anionic phospholipid vesicles [19]. Moreover, alkylation of the thiol group in the C-terminal cysteine at position 21 in the ShB peptide derivatives does not significantly alter either the conformational properties or the ability to restore inactivation in the deletion mutant ShBΔ6-46 K^+ channel compared with that exhibited by the wild-type ShB peptide [25]. We are now reporting fluorescence resonance energy transfer studies using NBD-labelled peptides as energy donors and rho-labelled peptides as energy acceptors (Table 1) to examine whether these peptides self-associate within the bilayer provided by PA vesicles. To optimize the fraction of peptide bound to the vesicles, the peptide to phospholipid molar ratios used in these experiments were within the exponential and the initial 'plateau' regions in the isotherms corresponding to the binding of either one of the peptides to PA vesicles [19]. Figure 1 shows that the addition of rho-labelled ShB peptide to NBD-labelled ShB peptide (panel A) and of rho-labelled ShB-L7E peptide to NBD-labelled ShB-L7E peptide (panel B) in the presence of PA vesicles determines a significant quenching of the donor emission and increases the acceptor emission, which is consistent with the occurrence of energy transfer. Control experiments in the absence of PA vesicles resulted in practically no fluorescence emission of the NBD-peptides (results not shown), which have a low quantum yield in hydrophilic media (see [26] and references therein). Therefore the observed energy transfer in the presence of PA vesicles originates from lipid-associated NBD peptides acting as

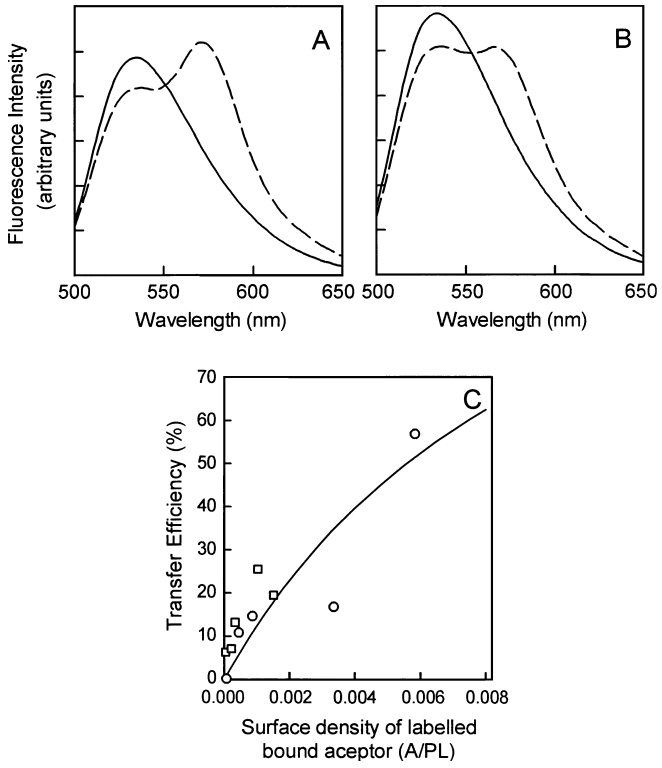

Figure 1 Fluorescence resonance energy transfer between NBD- and rho-labelled peptides in the presence of small unilamellar PA vesicles

(**A**) and (**B**) show examples of fluorescence energy transfer between ShB-NBD and ShB-rho peptides (**A**) and ShB-L7E-NBD and ShB-L7E-rho peptides (**B**), as described in Materials and methods. In these examples, the PA concentration was 150 μM, whereas the peptide/phospholipid ratio was 1:500. The continuous lines in (**A**) and (**B**) correspond to the emission of the NBD-labelled peptide donors alone, while the discontinuous lines correspond to the emission exhibited by the donor/acceptor labelled peptide mixtures. (**C**) Shows a plot of the experimentally determined efficiencies of energy transfer for both ShB-NBD and ShB-rho peptides (○) and ShB-L7E-NBD and ShB-L7E-rho peptides (□) donor/acceptor pairs, versus the bound-acceptor/phospholipid (A/PL) molar ratios. The continuous line in (**C**) shows the efficiencies of energy transfer expected from a random distribution of fluorescence peptide monomers assuming an R_0 of 50 Å [26].

energy donors. To determine the efficiency of the energy-transfer process, the amounts of the lipid-bound acceptors (the rho-peptides) in each experiment were calculated from the binding isotherms of the corresponding NBD-labelled peptides reported previously [19]. A plot of the experimentally determined percentages of energy transfer for both donor/acceptor pairs versus the bound-acceptor/phospholipid molar ratios is shown in Figure 1(C). Since the R_0 value (the distance at which the efficiency of the energy-transfer process is 50%) for the NBD/rho donor/acceptor pair is 51 Å [26], a curve showing the efficiencies of energy transfer expected from a random distribution of fluorescent-peptide monomers assuming an R_0 of 50 Å [26], is also included in Figure 1(C). It can be observed that the experimentally determined transfer efficiencies between NBD- and rho-labelled ShB peptides resemble closely those expected from a purely random distribution of peptide monomers at all the different bound-acceptor/phospholipid molar ratios examined. Oligomerization of other membrane-bound peptides, as determined by this technique, produces a large increase (approx. 6–7-fold) in the efficiency of the energy-transfer process compared to that expected from the random distribution of peptide monomers ([27] and references therein). Therefore, it can be concluded that the ShB peptide distributes randomly as peptide monomers throughout the PA membrane, rather than self-associating into oligomers.

As to the NBD- and rho-labelled ShB-L7E peptide derivatives, the experimentally determined transfer efficiencies for this donor/acceptor pair are always slightly above those expected from their random distribution in the vesicles (Figure 1C). This suggests that the mutant, non-inactivating ShB-L7E peptide has a small but detectable tendency to self associate under these conditions, which seems consistent with the observation that the mutant ShB-L7E peptide formed aggregates in the presence of anionic phospholipid vesicles, in a peptide-concentration-dependent manner [18].

The possibility of self-association of ShB or ShB-L7E peptides within the PA membranes was also tested by examining the monomer/excimer fluorescence emission ratios exhibited by pyr-labelled peptides (Table 1). Similarly to the observations with the NBD peptides from above, the pyr-peptides have a low quantum yield in aqueous solution and indeed, experiments in the absence of PA vesicles result in practically no fluorescence emission, thus indicating that the fluorescence recorded in the presence of PA vesicles originates from lipid-associated pyr peptides. Self-association of membrane-bound pyr-labelled peptides into oligomers should give raise to the formation of excited-state pyrene dimers (excimers) that exhibit a large characteristic component in the emission spectrum at about 480 nm, resulting in reported monomer/excimer emission ratios of 0.5 or higher [28]. In our samples, however, addition of either pyr-ShB or pyr-ShB-L7E peptides to PA vesicles at peptide/phospholipid ratios identical to those used in the above fluorescence energy transfer studies does not result in significant pyrene-excimer formation (Figure 2). Indeed, the small excimer emission, observed only at high peptide/phospholipid ratios, corresponds to monomer/excimer emission ratios equal or lower than 0.05 for either the ShB- or the ShB-L7E-labelled peptides, which indicates an almost exclusive occurrence of pyrene monomers.

Freeze–fracture studies of peptide insertion into phospholipid membranes

Previous studies using differential scanning calorimetry and synthetic dimiristoyl phospholipids demonstrated that the ShB peptide inserts readily into the hydrophobic domains of anionic phospholipid bilayers, while the mutant ShB-L7E peptide does not [19]. Those studies, however, did not inform as to how deep into the bilayer the insertion of the ShB peptide proceeded. We now report freeze–fracture electron-microscopical studies aimed at providing further support for the ShB peptide insertion phenomena and, most of all, to determine the depth of such insertion. Analysis of freeze–fracture replicas from either egg PC or PA vesicles, in the presence and in the absence of either ShB or ShB-L7E peptides, shows that globular intramembrane particles (IMPs) are observed only in the ShB peptide/PA vesicle samples (Figure 3B). Moreover, the IMPs observed in these samples appear at the same numerical density at both the exoplasmic and the protoplasmic fracture faces of the PA vesicles (means $\pm$ S.D.; 17 ± 2 and 20 ± 2 IMPs/10 μm^2, respectively). Since the peptide only incorporates into the preformed vesicles from the extravesicular aqueous side, we interpret its appearance at the same densities in both hemilayers of the replicas as a consequence of a deep insertion of the ShB peptide into the PA membrane. Other possible explanations for these observations, such as flip-flopping of the incorporated peptides between the two hemilayers, is considered highly unlikely because these experi-

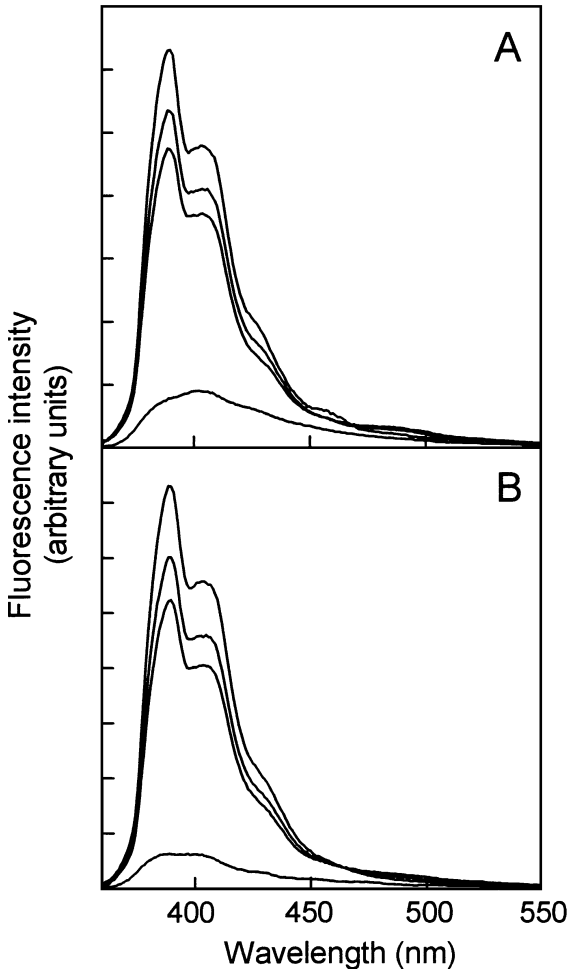

Figure 2 Fluorescence emission spectra of 0.3 μM solutions of pyr-labelled ShB (A) or pyr-labelled ShB-L7E (panel B)

Readings taken in the absence (bottom trace in each panel) or in the presence of increasing amounts of small unilamellar PA vesicles [15, 30 and 150 μM, in each of the three traces of increasing intensity on (**A**) or (**B**)]. Excitation at 345 nm.

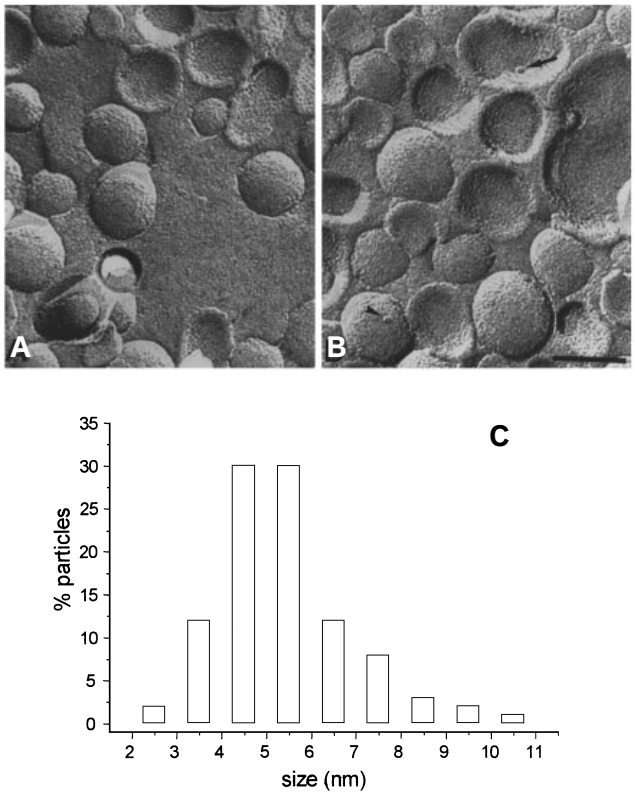

Figure 3 Electron micrographs of freeze–fracture replicas from plain small unilamellar PA vesicles (A) and from the same vesicles incubated in the presence of ShB peptide (B)

The arrows included in (**B**) indicate the presence of IMPs at both the protoplasmic and exoplasmic faces in the latter freeze–fracture replicas. Both micrographs were taken at the same magnification (scale bar, 50 nm). (**C**) Shows the size distribution of the IMPs observed in those samples ($n = 85$). The number of particles were recorded within a calibrated test square grid, superimposed on photographic prints of the freeze–fracture membrane. The size of all the IMPs inside the test square was measured using a calibrated eyepiece. The diameter recorded was the length of the base of the triangular shadow projected by the particle, perpendicular to the direction of the shadow. Since the angle of platinum shadowing with respect to the variable curvature of fracture faces may introduce changes in the apparent size of the particles, only flat regions of the membrane, with similar shadowing, were selected for quantitative analysis.

ments are carried out at very low peptide/phospholipid ratios, so that the external phospholipid leaflet at which the peptide incorporates from the aqueous media is far from being saturated. Also, the strongly cationic nature of the C-terminal end of the peptide should prevent it from traversing the anionic PA vesicle surface and the hydrophobic bilayer, as required by the flip-flop mechanism. Quantitative assessment of the IMPs observed in the replicas reveals an average size of 5.4 ± 1.6 nm (mean diameter $\pm$ S.D., $n = 85$). Moreover, the observed size distribution (Figure 3C) suggests that the ShB peptide assembles primarily as a single type of peptide-containing structure when embedded in the PA membrane matrix.

IMPs were never observed in control plain-phospholipid vesicles, demonstrating that IMP formation requires the presence of peptide. Furthermore, the lack of IMPs in samples from either (i) ShB or ShB-L7E peptides and PC vesicles, or (ii) ShB-L7E peptide and PA vesicles (Figure 3A) is consistent with the lack of insertion of the mutant ShB-L7E peptide into either PC or PA vesicles, as well as with the lack of insertion of the ShB peptide in PC vesicles seen previously by differential scanning calorimetry [19].

Trypsin hydrolysis studies of peptide location within PA vesicles

The ShB peptide contains four potential trypsin cleavage sites located near its C-terminal end (R14, R17, K18 and K19). We reported previously that trypsinization of the ShB peptide in solution at basic pH removes residues 15–20 at the C-terminus, leaving the remaining ShB 1–14 peptide unable to adopt the characteristic β-structure when challenged by anionic lipid vesicles [18]. Here we used trypsin hydrolysis to explore whether those potential tryptic sites remain accessible to polymer-immobilized trypsin added to the extravesicular aqueous medium, once the peptide is inserted into the PA vesicles. Again, the samples used in these experiments were prepared from preformed PA vesicles and added ShB peptide at a low peptide/phospholipid ratio to optimize the fraction of peptide bound to the vesicles from the aqueous media. Additionally, the samples were washed by centrifugation prior to the trypsin treatment to eliminate free peptide remaining in solution. It should also be noted that we have chosen neutral pH conditions in these studies, even though trypsin activity is not optimal at neutral pH. The reason for choosing those conditions is that the insertion of the ShB peptide

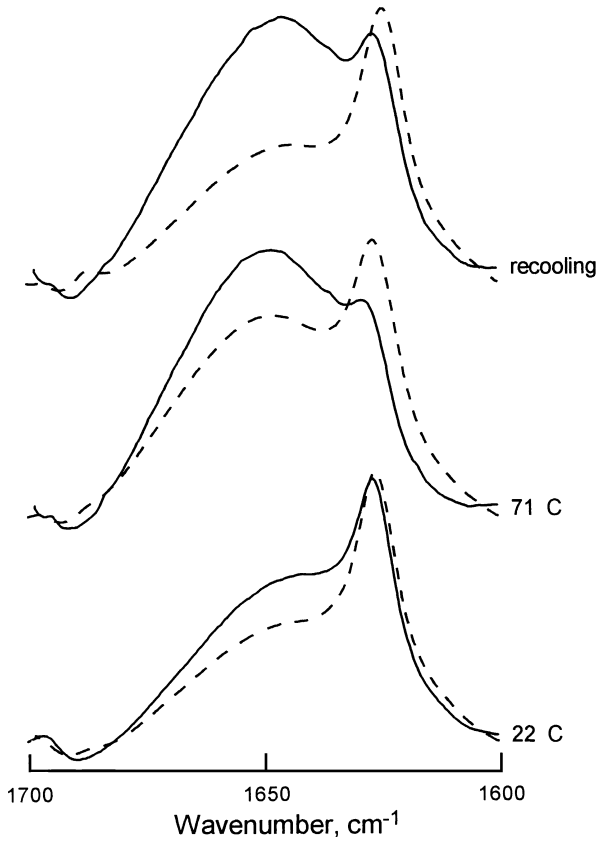

Figure 4 Effects of trypsin hydrolysis on the IR amide I band region in the original spectra of ShB peptide inserted into preformed small unilamellar PA vesicles

The spectra of non-hydrolysed control samples (broken line), as well as those of samples exposed to polymer-immobilized trypsin at pH 7.0 as described in Materials and methods (solid line), are shown. The lower traces represent spectra of samples taken at 20 °C, whereas the middle and upper traces correspond to samples heated at 70 °C in the spectrometer cell (heat-denatured samples) and to heated samples after recooling to 20 °C (renatured samples), respectively. In all cases, the spectra of the different buffers alone were subtracted from those of the peptide-containing samples.

into the vesicles does not occur above pH 8.5 [19], while it proceeds efficiently at neutral pH.

Figure 4 shows that the amide I band in the IR spectra of the ShB peptide inserted into PA vesicles becomes altered upon exposure to the polymer-immobilized trypsin at neutral pH. The main feature of such alteration is the reduction in the characteristic β-structure component at 1623 cm^{-1} in the spectra of trypsin-treated samples. Also, the remarkable thermal stability exhibited normally by the vesicle-inserted ShB peptide, as well as its ability to almost completely regain its native conformation upon cooling of previously heated samples [18,19], are greatly decreased upon exposure to the polymer-immobilized trypsin (middle and upper traces in Figure 4). The reported spectral alterations were clearly more noticeable at pH 7.5 than at pH 7.0, indicating that the increase in trypsin activity upon increasing the pH was responsible for the observed effects. These results suggest that some, if not all, of the four potential tryptic sites near the C-terminus of the vesicle-inserted ShB peptide remain accessible to attack by polymer-immobilized trypsin.

Attempts to use conventional, reversed-phase HPLC/amino acid-analysis methods to identify the tryptic peptides failed because the large amounts of lipid present in these samples interfered greatly with the HPLC separation. For this reason, we turned to MS in an attempt to identify the hydrolysis products based on their molecular mass. Control ShB peptide-vesicles samples prepared in the absence of trypsin show a single component with a molecular mass of 2226 Da, corresponding to the entire ShB peptide (expected molecular mass of 2227.6 Da, [18]). Also, control samples corresponding to plain phospholipid vesicles prepared in the presence of trypsin did not show any components in the 1000–2500 Da molecular-mass window. On the other hand, ShB peptide-vesicle samples that were incubated at pH 7.0 with trypsin and processed, as described under the Materials and methods section, show two components of molecular mass 1420 and 2226 Da, respectively. While the 2226 Da component corresponds to the entire ShB peptide that remains undigested because of the poor activity of trypsin at pH 7.0, the 1420 Da component matches closely the expected mass of the ShB 1–14 peptide fragment (calculated as 1421.7 Da). No other components of molecular mass within the 1420 and 2226 Da values were detected, thus suggesting that at least the trypsin-cleavage site at the R14 in the ShB peptide sequence remains accessible to polymer-immobilized trypsin after insertion of the peptide in the model vesicle target.

DISCUSSION

Previous studies on the interaction between the K^+ channel-inactivating ShB peptide and anionic phospholipid vesicles as a model target have shown that the inactivating ShB peptide: (i) binds to the vesicle surface with a relatively high affinity; (ii) readily adopts a strongly hydrogen-bonded β-structure; and (iii) becomes partly or totally inserted into the hydrophobic bilayer in a pH-dependent manner [19]. Moreover, FTIR monitoring of the adoption of β-structure by the ShB peptide shows a lack of dependence of such a conformation on the concentration of peptide, at least within the range of peptide concentrations used in these studies [18]. This suggests that the observed β-structure could be intramolecular. Nonetheless, the peptide concentrations required by FTIR are high in absolute terms, and the possibility that the peptide is always aggregated under those conditions and that the observed β-structure results from intermolecular hydrogen bonding cannot be excluded solely on the basis of FTIR data. In the studies presented here we have investigated the state of aggregation of the vesicle-bound ShB peptide by using fluorescent-peptide derivatives that allow the use of concentrations much lower than in FTIR. Fluorescence resonance energy transfer measurements using NBD-labelled ShB peptide as the energy donor and rho-labelled ShB peptide as the energy acceptor (Figure 1), as well as measurements of excimer formation using pyr-labelled ShB peptide (Figure 2), strongly suggest that the vesicle-inserted peptide is in a monomeric form and does not self-assemble into oligomers at any of the peptide/phospholipid ratios used in these studies. The observation of a monomeric form of the ShB peptide when complexed with the anionic-vesicle model target implies that the highly stable β-structure adopted readily by the ShB peptide on interaction with the anionic phospholipid vesicles [18] results from intramolecular hydrogen bonding within the monomeric ShB peptide. This requires that the ShB peptide folds as a β-hairpin-like structure in which the more likely candidate to account for the necessary β-turn is one of the glycine residues at positions 6 or 9 in the peptide sequence, due to steric reasons as well as the larger degree of rotational freedom. In this respect, the freeze–fracture and trypsin-hydrolysis studies provide additional information to help dis-

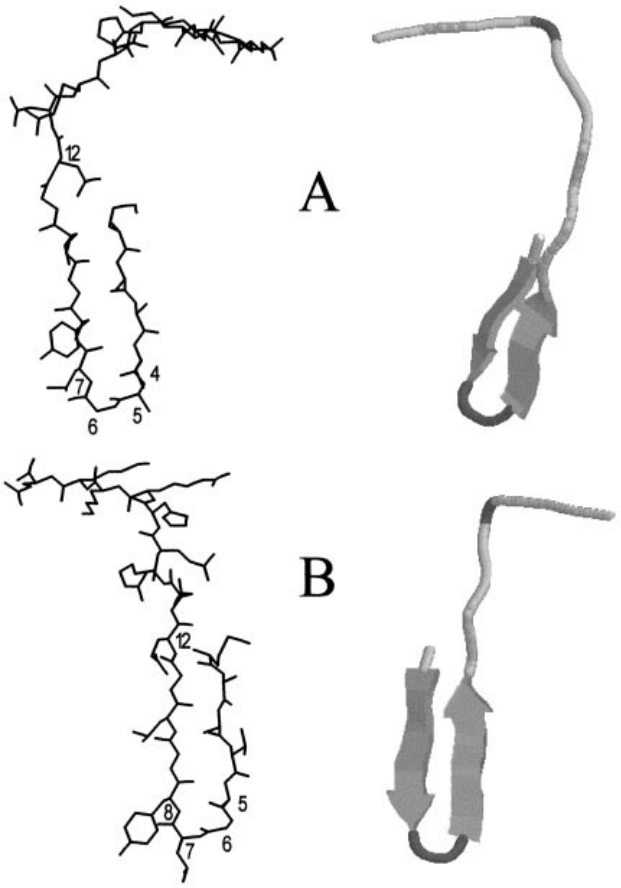

Figure 5 Alternative models of the β-hairpin proposed for the ShB peptide inserted into anionic phospholipid vesicles

The required β-turn has been formed by either the VAGL (**A**) or the AGLY (**B**) tetrapeptide sequences (amino acids 4–7 or 5–8 in the ShB peptide sequence). Numbers within the figures in the more detailed structures on the left indicate the positions of the corresponding β-carbons. The diagrams on the right are simplified representations of the same hairpins. Modelling of the peptide was carried out in a Silicon Graphics work station using the program Sybyl (Tripos Inc., St. Louis, MO, U.S.A.). The backbone torsion angles for residues 5 and 6 (**A**) or residues 6 and 7 (**B**) were manipulated to allow proper hydrogen-bonding between the two extended strands. The backbone angles for all the other residues were set to standard values of an extended structure. The resulting hairpin structures were submitted to an energy minimization procedure with the Sybyl force field.

tinguish which of the proposed β-folds is more likely to take place. First, freeze–fracture images indicate that the ShB peptide added to the extravesicular aqueous medium inserts deeply enough into the vesicle bilayer as to perturb both hemilayers simultaneously (Figure 3). Secondly, the C-terminal portion of the deeply inserted ShB peptide remains accessible to hydrolysis by trypsin added to the extravesicular side (Figure 4) and was located at or near the membrane surface upon insertion [19], which is consistent with previous studies on binding of NBD-labelled ShB peptide to anionic phospholipid vesicles in which the NBD-reporter group was covalently attached to the peptide C-terminus. The above results require that the folded β-structure be long enough to practically traverse a hemilayer while maintaining the C-terminus containing the potential tryptic cleavage sites exposed to the aqueous media and, therefore, the longer β-hairpin resulting from a fold involving G6 appears to be a more likely candidate than the shorter one resulting from a turn at G9. It could also be reasonably argued that the deep insertion of the folded peptide into the hydrophobic bilayer requires that the net charges present in the inserted portion of the peptide sequence be somehow cancelled (i) to enable the peptide to traverse the anionic interphase formed by the phospholipid polar head groups and (ii) to stabilize the hydrophobic interactions maintaining the inserted peptide in place. According to this idea, we would expect that folding of the ShB peptide as a β-hairpin brings charged amino acid residues of different signs closer together, thus favouring the formation of salt bridges and contributing to the remarkable stability exhibited by the resulting β-structure.

These experimental findings and conclusions have been used in building plausible structural models for the vesicle-inserted ShB peptide. Figure 5 shows two such possible structures that conform sufficiently well to the experimental observations. In such models, the required β-turn has been formed by either the 4–7 (VAGL) or the 5–8 (AGLY) tetrapeptide sequences. The VAGL turn (Figure 5A) has a higher probability of forming a β-turn, according to Chou and Fasman's predictions [29], and leaves the M1 and E12 residues sufficiently close to each other to form a salt bridge between their N-terminal amine and side-chain carboxyl groups, respectively. The stability of this structure should be further increased by the hydrophobic interaction resulting from confrontation of the two hydrophobic V4 and L7 residues in the hairpin. On the other hand, the AGLY turn (Figure 5B) produces a longer hairpin with more extensive hydrogen-bonding and brings the M1 and E12 residues much closer together. In both structures shown in Figure 5 an additional salt bridge between the D13 and R14 side chains has been introduced to produce a complete internal cancellation of net charges in the chain stretch comprising amino acids 1–16. As to the positively charged C-terminal portion of the ShB peptide, it has been modelled parallel to the membrane surface and as extended as possible to facilitate its electrostatic interaction with the negatively charged head group of PA.

The observation of 'crossed inactivation' between channel proteins and inactivating peptides of different origins (see the Introduction) has suggested that channel inactivation occurred as a consequence of the interaction between complementary domains, relatively unconstrained in terms of their primary structure, present in the two interacting molecules. As stated previously [19], this conclusion makes it conceivable that the interaction of the inactivating peptide with the model vesicle target, which also contains an anionic surface and a hydrophobic region as defined domains, could partly imitate the association of the peptide with the corresponding receptor site in the inactivation entrance of the real channel protein. Assuming the above, one would predict that the conformation adopted by the inactivating peptide bound to the channel protein should also be somewhat similar to that seen in the model vesicle target. In any case, the proposed models could be further tested to see whether they fit existing data. For instance, the models propose that the ShB peptide organizes as a monomer when confronted with its target. This seems in agreement with reports showing that channel inactivation results from the interaction of a single ShB peptide with the corresponding receptor site on the channel protein [8,9]. Also, the models predict that introduction of net charges in the β-hairpin region of the monomeric peptide makes it energetically unfavourable to traverse an anionic interphase and to insert into the underlying hydrophobic domain. This is exactly the case for the peptide mutants ShB-L7E and ShB-L7R (negatively and positively charged, respectively, at their corresponding β-hairpin regions), both of which were found to be non-inactivating peptide variants [2]. Moreover, the proposed models and the relative location of amino acid residues seem consistent with the only

piece of experimental information on the conformation of the channel-bound peptide [15] which, based on the kinetics of channel inactivation caused by peptide mutants, proposed an 'extended' peptide conformation in which the L7 side chain is more effectively buried in a hydrophobic region of the channel protein than the side chain of L10. On the other hand, the observation that the double mutant ShB-E12K-D13K, in which the salt bridges postulated in the model could not be formed, is an effective inactivating variant of the ShB peptide [15] suggests that insertion of the peptide in the internal channel mouth may not be as deep as that seen in the model vesicle target. In relation to this, we reported previously that in the interaction of the peptide with sodium cholate micelles, in which the extent of peptide insertion is limited by micellar size, the peptide still retains the ability to adopt β-structure [18]. Nevertheless, it should be emphasized that there are intrinsic difficulties and limitations for most simple models to mimic precisely the more complicated components in biological systems and, therefore, predictions from model systems should be taken as a reasonable guess on the behaviour and properties that real molecules are likely to exhibit.

We are grateful to L. M. García-Segura for his help with the freeze–fracture studies, to C. Gonzalez, G. Lunt and J. Schmitt for their help and comments on the computer modelling of the peptide and to E. Camafeita and E. Mendez for the MS analysis. This work was supported partly by grants from the DGICYT of Spain (PM95-0108, PB93-0934 and PB93-0093). J. A. E. is a recipient of a predoctoral fellowship from the Ministerio de Educación y Ciencia of Spain.

REFERENCES

1 Armstrong, C. M. and Bezanilla, C. F. (1977) J. Gen. Physiol. **70**, 567–590
2 Hoshi, T., Zagotta, W. N. and Aldrich, R. W. (1990) Science **250**, 533–538
3 Zagotta, W. N., Hoshi, T. and Aldrich, R. W. (1990) Science **250**, 568–571
4 Jan, L. Y. and Jan, Y. N. (1992) Annu. Rev. Physiol. **54**, 537–555
5 Li, M., Unwin, N., Stauffer, K. A., Jan, Y. N. and Jan, L. Y. (1994) Curr. Biol. **4**, 110–115
6 Catterall, W. A. (1995) Annu. Rev. Biochem. **64**, 493–531
7 Li, M., Jan, Y. N. and Jan, L. Y. (1992) Science **257**, 1225–1230
8 MacKinnon, R., Aldrich, R. W. and Lee, A. W. (1993) Science **262**, 757–559
9 Gomez-Lagunas, F. and Armstrong, C. M. (1995) Biophys. J. **68**, 89–95
10 Isacoff, E. Y., Jan, Y. N. and Jan, L. Y. (1991) Nature (London) **353**, 86–90
11 Dubinsky, W. P., Mayorka-Wark, O. and Schultz, S. (1992) Proc. Natl. Acad. Sci. U.S.A. **89**, 1770–1774
12 Toro, L., Stefani, E. and Latorre, R. (1992) Neuron **9**, 237–245
13 Foster, C. D., Chung, S., Zagotta, W. N., Aldrich, R. W. and Levitan, I. B. (1992) Neuron **9**, 229–236
14 Kramer, R. H., Goulding, E. and Siegelbaum, X. (1994) Neuron **12**, 655–662
15 Murrell-Lagnado, R. D. and Aldrich, R. W. (1993) J. Gen. Physiol. **102**, 949–975
16 Patton, D. E., West, J. W., Catterall, W. A. and Goldin, A. L. (1993) Neuron **11**, 967–974
17 Kukuljan, M., Labarca, P. and Latorre, R. (1995) Am. J. Physiol. Cell Physiol. **268**, C535–C556
18 Fernandez-Ballester, G., Gavilanes, F., Albar, J. P., Criado, C., Ferragut, J. A. and Gonzalez-Ros, J. M. (1995) Biophys. J. **68**, 858–865
19 Encinar, J. A., Fernandez, A. M., Gavilanes, F., Albar, J. P., Ferragut, J. A. and Gonzalez-Ros, J. M. (1996) Biophys. J. **71**, 1313–1323
20 Surewicz, W. K., Mantsch, H. H. and Chapman, D. (1993) Biochemistry **32**, 389–394
21 Zhang, Y-.P., Lewis, R. N. A. H., Hodges, R. S. and McElhaney, R. N. (1992) Biochemistry. **31**, 11572–11578
22 Kyaw, A., Maung, U. H. and Toe, T. (1985) Anal. Biochem. **145**, 230–234
23 Mendelsohn, R. and Mantsch, H. H. (1986) in Progress in Protein-Lipid Interactions (Watts, A. and DePont, A., eds.), pp. 103–146, Elsevier Science, Amsterdam
24 Castresana, J., Fernandez-Ballester, G., Fernandez, A. M., Laynez, J. L., Arrondo, J. L. R., Ferragut, J. A. and Gonzalez-Ros, J. M. (1992) FEBS Lett. **314**, 171–175
25 Fernandez, A. M., Molina, A., Encinar, J. A., Gavilanes, F., Lopez-Barneo, J. and Gonzalez-Ros, J. M. (1996) FEBS Lett. **398**, 81–86
26 Peled, H. and Shai, Y. (1993) Biochemistry **32**, 7879–7885
27 Fung, B. K.-K. and Stryer, L. (1978) Biochemistry **17**, 5241–5248
28 Morris, S. J., Bradley, D., Gibson, C. C., Smith, P. D. and Blumenthal, R. (1988) in Spectroscopic membrane probes (Loew, L. M., ed.), pp. 161–191, CRC Press, Boca Raton, Florida
29 Chou, P. Y. and Fasman, G. D. (1978) Annu. Rev. Biochem. **47**, 251–276

Received 1 September 1997/23 December 1997; accepted 16 January 1998